An instrument to measure and speciate the total reactive nitrogen budget indoors: description and field measurements

Leigh R. Crilley[1], Melodie Lao[1], Leyla Salehpoor[1], and Trevor C. VandenBoer[1,*]

[1] Department of Chemistry, York University, Toronto, ON, Canada.

[*]Correspondence to: tvandenb@yorku.ca

Abstract

Reactive nitrogen species (N_r), defined here as all N-containing compounds except N_2 and N_2O, have been shown to be important drivers for indoor air quality. Key N_r species include NO_x ($NO+NO_2$), HONO and NH_3, that are known to have detrimental health effects. In addition, other N_r species that are not traditionally measured may be important chemical actors for indoor transformations (e.g. amines). Cooking and cleaning are significant sources of N_r, whose emission will vary depending on type of activity and materials used. Here we present a novel instrument that measures the total gas-phase reactive nitrogen (tN_r) budget and key species NO_x, HONO, and NH_3 to demonstrate its suitability for indoor air quality applications. The tN_r levels were measured using a custom-built heated platinum (Pt) catalytic furnace to convert all N_r species to NO_x, called the tN_r oven. The measurement approach was validated through a series of control experiments, such that quantitative measurement and speciation of the total N_r budget is demonstrated. The optimum operating conditions of the tN_r oven were found to be 800 °C with a sampling flow rate of 630 cubic centimetres per minute (ccm). Oxidized nitrogen species are known to be quantitatively converted under these conditions. Here, the efficiency of the tN_r oven to convert reduced N_r species to NO_x was found to reach a maximum at 800 °C, with 103 ± 13% conversion for NH_3 and 79-106% for selected relevant amines. The observed variability in conversion efficiency of reduced N_r species demonstrates the importance of catalyst temperature characterization for the tN_r oven. The instrument was deployed successfully in a commercial kitchen, a complex indoor environment with periods of rapidly changing levels and shown to be able to reliably measure the tN_r budget during periods of longer-lived oscillations (>20 mins), typical of indoor spaces. The measured NO_x, HONO and basic N_r (NH_3 and amines), were unable to account for all the measured tN_r, pointing to a substantial missing fraction (on average 18%) in the kitchen. Overall, the tN_r instrument will allow for detailed survey(s) of the key gaseous N_r species across multiple locations and may also identify missing N_r fractions, making this platform capable of stimulating more in-depth analysis in indoor atmospheres.

Environmental Significance Statement

Indoor air is increasingly being recognized as being chemically complex, and our understanding of the chemical process driving poor indoor air quality are lacking. People and their activities emit a range of compounds that affect indoor air quality, and thus there is a need for new tools that can do detailed chemical measurements yet remain unobtrusive for occupant exposure assessments. Here we describe

a novel instrument to address an existing gap for reactive nitrogen species, a key driver of indoor air quality, that will allow for more detailed and widely conducted surveys of indoor environments. This approach may identify overlooked nitrogenous species of importance, leading to more rapidly improved indoor air quality outcomes.

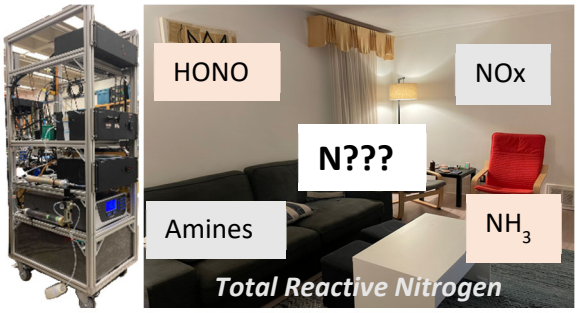

1.0 Introduction

Reactive nitrogen species (N_r) are here defined as all atmospheric nitrogen compounds except for N_2 and N_2O. In the gas-phase, this includes nitrogen oxides (NO + NO_2, collectively referred to as NO_x) as well as the reservoir species of NO_x (NO_z; NO_3 + N_2O_5 + HONO + HNO_3 + peroxy and alkyl nitrates (e.g. $RONO_2$)). Collectively, the sum of NO_x and NO_z species is referred to as NO_y. Note that while HCN, NH_3 and amines (e.g. trimethyl amine) are generally not considered as NO_y species as they are not NO_x reservoirs, they are considered as N_r due to their chemical reactivity in the atmosphere [1–3]. N_r can also be found in the particle-phase and include organic and inorganic nitrogen species, such as ammonium nitrate (NH_4NO_3). Outdoors, N_r plays a significant role in atmospheric chemistry, radiative balance, air quality, and nitrogen deposition in both terrestrial and aquatic ecosystems[4–8].

While ammonium (NH_4^+) and nitrate (NO_3^-) are important for aerosol chemistry outdoors, indoors the concentration of these species in the particle phase are typically very low, with the majority of airborne particles organic[9,10]. For example, Omelekhina et al.[10] in a residential home observed very low NH_4^+ and NO_3^- particle levels, at 0.3 and 0.2 μg m^{-3}, or 2% of the total PM_1 (15 ug m^{-3}) mass loading, respectively. Levels of airborne particles indoors are typically lower compared to outdoors, due to physical losses such as deposition to surfaces and filtration in building ventilation systems[11,12]. Emissions of particle-bound nitrogen containing organic compounds (e.g. heterocyclic aromatic amines) have been observed during meat cooking[13,14], and as such these could be important short-lived considerations for indoor air quality during such activities. Levels of particle-phase NH_4^+ and NO_3^-, in contrast, are further depleted relative to other aerosol components (e.g., SO_4^{2-}) owing to their higher volatility and as such underdo thermodynamically driven partitioning to the gas phase or redistribution onto indoor surfaces[12,15]. Overall, these results suggest that indoors the contribution of traditional particle bound N_r species to the total budget are likely transient, generally small, and in some cases may be negligible. In contrast, gas-phase N_r have been shown to important drivers for indoor air quality, with key species including NO_x, HONO and NH_3, which are all known to have detrimental health effects and are chemically reactive. Consequently, the focus in the current work is on the gas-phase fraction of all indoor N_r species.

Concentrations indoors of many key gas-phase N_r species - known to control outdoor chemistry and secondary pollutant levels - can exceed outdoor levels by a several orders of magnitude, driven by direct sources and surface reservoirs [16]. Surface reservoirs play a key role in controlling levels of reactive species

indoors. The surface area to volume ratio indoors is much higher than outdoors, making many species that would be considered volatile under typical outdoor conditions exhibit semi-volatile characteristics indoors[17]. For example, gases like HONO and NH_3 participate in dynamic surface-gas partitioning and multi-phase chemistry on surfaces, that are governed in part by room ventilation rates and also chemistry of the surfaces[18,19].

Direct indoor sources of N_r include combustion, such as gas stoves or candle burning, which emit significant quantities of NO_x and HONO[18]. There are several direct sources of NH_3 indoors, including smoking, building materials, cooking and cleaning. Humans, from breath and dermal emissions, can be one of the more significant sources of indoor NH_3 ([20] and references therein). Emissions of nitrogen containing volatile organic compounds (VOCs) have been observed during protein cooking in oil[14], during cleaning[21–23] and from building materials (carpet and drywall)[24]. Cleaning and cooking emissions are perhaps the most variable of direct sources indoors, as it depends on the type of activity and materials used. Emissions from cooking depend in part on the type of food, with meat cooking a known source of NH_3 thought to be derived from the breakdown of amino acids [19], while fish cooking can emit amines[25,26]. Emissions also vary by cooking method, as demonstrated by the recent HOMEChem campaign[27]. For example, combustion cooking methods (gas stove and oven) emitted elevated levels of HONO and NO_x, compared to cooking on an electric hot plate [18]. Cleaning emissions depend on the active ingredient in a given cleaning product, which can include NH_3, vinegar (i.e. dilute $HCOOH/HCOO^-$) or bleach (i.e. dilute $HOCl/OCl^-$). Cleaning emissions can include direct volatilization of the active ingredient, or can drive the partitioning of basic and acidic species (e.g. NH_3 and HONO) from surfaces by changing the pH of surfaces reservoirs[17,18]. Cleaning with HOCl can facilitate reactions with NH_3 to form toxic chloramines in surprisingly significant quantities. Quantification of chloramines remains problematic, but it is likely that they are present in cleaning-impacted indoor air in the ppbv range[21,22,28]. There may be other N_r species, such as amines in both the gas- and particle-phase that are not traditionally measured outdoors due to analytical challenges from very low concentrations[29,30], that may be important chemical actors for indoor transformations. Given the potential for stronger sources and novel chemistry, understanding the total budget of gas-phase N_r species indoors will further our understanding of chemistry in such spaces, which are as varied as the humans that use them.

An established and robust method for quantifying N_r species is by thermal and catalytic conversion at high temperatures. The N_r is converted to primarily NO along with small amounts of NO_2, with subsequent measurement by a chemiluminescent NO_x analyser (See e.g. [31–33]). This method can be applied for the quantitative conversion of both gas- and particle-phase N_r species, with near unity conversion efficiency demonstrated[31,33]. Commercial instruments exist that utilise this approach, primarily for speciating NH_3 and NO_x (e.g., Thermo Scientific 17i). Examples of total N_r budget measurements previously in the literature include during controlled burn laboratory experiments[3], agricultural fluxes[33,34] and near forests[35]. Overall, catalytic conversion of N_r species in both gas and condensed phases for measurement by a NO_x chemiluminescent analyser has been successfully applied for quantitively determining the total N_r budget in ambient outdoor settings.

The current state of instrumentation to measure N_r budget were developed for outdoor research, which are not always suitable for indoor measurements, due to instrumentation size, cost and/or containing hazardous components. To avoid these issues, passive samplers and denuders have been previously used for indoor measurements of many key N_r species[36–39]. While allowing for large-scale deployment to conduct society-wide surveys, the time response of these offline methods is often lengthy (i.e. hours to

days). Many key N_r species have lifetimes on the order of 100-1000 seconds and depending on air exchange rates (e.g. NH_3 and HONO), meaning that an instrument with high time resolution is required to capture the temporal variability of such moderately lived species.[40]. New instrumentation is needed to bring the capabilities of outdoor instrumentation indoors to obtain an accurate determination of the emissions and transformations of N_r species. This is paramount as surveys require indoor environments to be used as they normally would be by occupants[41]. The instrument deployed in indoor environments must also be unobtrusive for occupants with respect to noise (e.g. vacuum pumps), basic concerns around physical hazards (e.g. tripping, heat), and advanced safety considerations (e.g. no hazardous reagents/waste).

Here we describe a high time resolution instrument to measure and speciate the total gas-phase N_r budget and demonstrate its suitability for indoor air quality applications. The instrument is validated by a series of positive and negative control experiments designed to evaluate the time response of the instrument with respect to key indoor N_r gas-phase species, namely NO, NO_2, HONO and basic N_r-species including NH_3 and amines. The ability of the instrument to quantitatively convert reduced N_r species (e.g., NH_3 and amines) to NO_x allows their quantitative measurement by a NO_x analyser. Within this demonstration, key controlling factors are identified and optimized. To demonstrate the capability of the instruments in the field, proof-of-concept measurements in a commercial kitchen are presented. The highly dynamic nature of emissions and sinks in this environment provide a robust test of the instrument capabilities to measure the total N_r and the acidic and basic fractions of its constituent species at high time resolution, with the first indoor total N_r budget analysis presented.

2.0 Method

2.1 Instrument Description

This instrument was designed to measure the total N_r (henceforth denoted as tN_r) budget and the contribution of key reactive nitrogen species, pooled by chemical classes of acids, bases, and neutral species through selective scrubbing. A schematic overview of the instrument is provided in Fig 1, with detailed description provided in the following sections. Briefly, Fig 1 indicates the different measurement pathways for determining the different N_r species prior to detection in a chemiluminescent NO_x analyser. The instrument has one sample inlet, which is then directed via one of two pathways. The first is for NO_x and the second for the tN_r measurement. Direction of the flow is controlled via 3-way solenoid valves, which are operated automatically with a microcontroller. The NO_x pathway enables measurement of NO_x and acidic N_r species (e.g., HONO and HNO_3) by difference, via selective scrubbing with a sodium carbonate (Na_2CO_3) coated annular denuder. For the tN_r measurement, an air sample is directed to the furnace containing pure platinum (Pt) mesh that facilitates the catalytic conversion of all N_r species to NO_x. Selective scrubbing in this pathway uses a denuder coated with phosphorous acid (H_3PO_3) prior to the furnace to allow for determination of levels of basic N_r species (e.g., NH_3 and amines). This fraction is calculated by difference compared to the tN_r measurement. Flows of calibration gases (e.g., HONO and NH_3) from their sources prior to entering the tN_r instrument is also controlled at the main sampling inlet. All the components shown in Fig 1 are housed in a standard 19" rack, with a complete description available in Section S1, Supporting Information (SI).

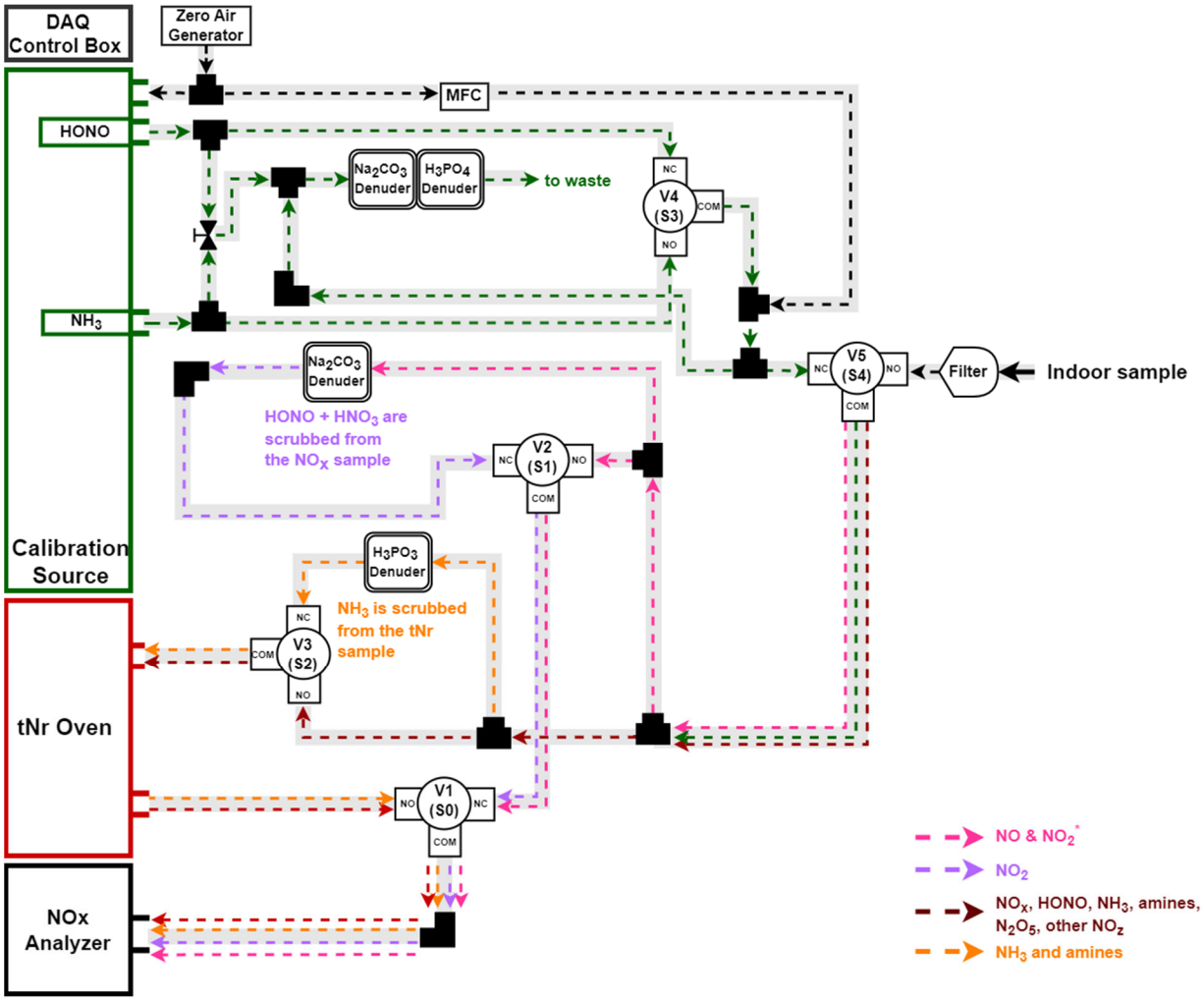

Fig 1. Schematic flow diagram of the measurement pathways in tN_r instrument. The different colours indicate the species or tN_r fraction selection points, described in detail in Table 1. Briefly, air enters the instrument through a filter, and is directed via the NO_x (pink) or tN_r (red) measurement pathway, to be measured by the NO_x analyser. Acids (purple) or bases (orange) are scrubbed by annular denuders. Green arrows indicate the flow of calibrations gases from the in-situ sources to the inlet. The flow of the gases can be directed by the three-way solenoid valves by entering either the normally open (NO) or nominally closed (NC) and exit through the common (COM) port.

2.1.2 NO_x measurement

A commercially available chemiluminescent NO_x analyser (Serinus 40, American Ecotech, Warren, RI) was employed to measure NO, NO_2 and NO_x. The manufacturer stated limit of detection for the NO_x analyser is 0.4 ppbv with a response time of 15 seconds to reach 90 % of maximum signal with a total sample flow of 0.63 standard litres per minute (slpm)[42], with the analyser precision during proof-of-concept measurements presented later. This NO_x analyser has two channels; one where the air sample is passed over a Mo catalyst to convert NO_2 to NO yielding a measure of NO_x (= NO + NO_2) and one that bypasses the catalyst to measure NO only. This NO_x analyser uses a heated molybdenum (Mo) convertor

(325 °C), known to convert other NO_y species (i.e. HNO_3, HONO, N_2O_5, HO_2NO_2, peroxyacetyl nitrate (PAN), NO_3 and organic nitrates[43,44]) to NO in addition to NO_2. Conversion of NO_y species on the Mo catalyst will vary between analysers, with our previous work demonstrating that this analyser has unity conversion[45]. The detection limit of HONO was determined experimentally by flushing the system with zero air and propagating the uncertainty in each of the NO_x and NO channels, which were determined to be 0.53 and 0.5 ppbv, respectively. These are slightly higher than noted by the manufacturer and will result from the extensive use of the instrumentation. Since the difference between these two channels determines NO_2, the calculated HONO detection limit that results is 0.73 ppbv at one minute time resolution. The NO_x analyser was calibrated regularly. Prior to the proof-of-concept measurements a full calibration was performed using a gas-calibration unit (Gascal 1100TS, American Ecotech, Warren, RI), a standard gas cylinder of NO (Praxair, NI NO5MC-A3, 4.88 (±5 %) ppmv, Toronto, ON), and gas-phase titration of NO to NO_2 with ozone (O_3).

2.1.3 Measurement of the total reactive nitrogen (tN_r) budget

To measure the tN_r budget, we used a custom-built heated Pt catalyst to convert the total N_r species to NO_x, as described in detail by Stockwell et al. [31]. Briefly, the Pt catalyst (99.9% Pt gauze mesh, 100 gauge, 1.7 g, 18 cm^2, Sigma-Aldrich) is packed within quartz tubing (0.5 inch OD) to maximise surface area over 10 cm length inside the tube, and heated to 800 °C. Stockwell et al. [31] demonstrated that a similar heated Pt catalyst (750°C) can convert both gas-phase and particle-bound N_r species quantitatively to NO_x. Here, we focus only gas-phase N_r species, as this is the primary focus for indoor measurements. To remove airborne particles a 47 mm polytetrafluoroethylene (PTFE) filter was installed at the inlet and was replaced regularly (weekly) during field measurements to avoid off-gassing of semi-volatile particle-bound N_r (e.g., NH_4NO_3). Throughout the remainder of this work, we refer to this component of the instrument as the tN_r oven.

2.1.4 Reactive nitrogen speciation by differential measurement

The instrument utilises four alternating pathways to selectively measure different N_r species (Fig 1). The NO_x analyser measures NO and NO_2 and total gas-phase N_r ($N_{r,gas}$) from the oven by their sum, while chemically selected N_r species are measured by difference through selective scrubbing with coated annular denuders (Fig 1, Table 1). Acidic N_r species ($N_{r,acid}$), which are primarily HONO and HNO_3 in the gas-phase indoors, were scrubbed using a Na_2CO_3 coating [46]. The Na_2CO_3 denuder was prepared according to the EPA Compendium Method IO-4.2[47] to remove atmospheric acids by reactive uptake to the basic coating. This scrubbing technique has been previously applied for indoor sampling and quantification of HONO[46]. Quantitative conversion of HONO and HNO_3 to NO occurs on the Mo catalyst of the NO_x analyser. Consequently, the measured NO_2 from an air sample passed through the Na_2CO_3 denuder will decrease proportionally to the amount of HONO and HNO_3 present.

Therefore, the $N_{r,acid}$ mixing ratio can be determined by difference according to Eqn 1:

$$N_{r,acid} = NO_2^* - NO_2 \qquad \text{(E1)}$$

Where NO_2^* is the sum of NO_2 and $N_{r,acid}$ species, and NO_2 is the correctly measured mixing ratio. Since HNO_3 mixing ratios are expected to be small indoors (e.g. low pptv range[48–50]), we expect that the $N_{r,acid}$ measurement can be equated to HONO with a high level of confidence. In addition, measured NO_2 through

the denuder will be closer to the true level of NO_2, as NO_z species that pass through the denuder and are converted by the Mo catalyst (e.g. alkyl nitrates) are also thought to be low indoors[51,52].

Gas-phase basic N_r species ($N_{r,base}$) were also selectively scrubbed, but using a denuder coated in H_3PO_3 [39] (Fig 1). On this instrument, these species can only be measured after conversion to NO_x in the tN_r oven. The mixing ratio of $N_{r,base}$ was determined by difference between $tN_{r,gas}$ and $tN_{r,scrubbed}$ by the H_3PO_3 denuder according to Eqn 2:

$$N_{r,base} = tN_{r,gas} - tN_{r,scrubbed} \quad \text{(E2)}$$

In the indoor environment, NH_3 is expected to be the dominant species in $N_{r,base}$ based on prior reports, but will also include contributions from other basic N_r compounds such as amines. In the indoor environment, typical amines include monomethylamine (MMA), dimethylamine (DMA), trimethylamine (TMA), monoethylamine (MEA), diethylamine (DEA) and triethylamine (TEA) [53,54]. An example time series of raw NO_x measurements for a single 20 minute duty cycle is shown in Fig S2 (Supporting Information).

Table 1. Overview of calculations for the different N_r species.

Species	Species measured	Calculation	Fig. 1 pathway	Eqn.
NO and NO_2^*	NO & NO_2^*	Ambient NO_x, NO_2 and NO	Pink (NO_x)	
NO_2	NO_2	Measured NO_2 after Na_2CO_3 denuder	Purple (Na_2CO_3 denuder)	
Acidic N_r ($N_{r,acid}$)	HONO & HNO_3	$NO_2^* - NO_2$	Pink (NO_x) – Purple (Na_2CO_3 denuder)	E1
Gas-phase total N_r ($tN_{r,gas}$)	NOx, HONO, NH_3, amines, N_2O_5, other NO_z	Measured NO_x after tN_r oven	Red (tN_r oven)	
Basic N_r ($N_{r,base}$)	NH_3 and amines	Measured NO_x after H_3PO_3 denuder and tN_r oven	Red (tN_r oven) – Orange (H_3PO_3 denuder)	E2

2.1.5 In-situ calibration source for HONO and NH_3

A custom-built calibration source of HONO and NH_3 was installed on the instrument to allow regular in-situ tests of the denuder scrubbing efficacy and the conversion efficiencies of the two analytes on the catalyst to ensure that the Na_2CO_3 and H_3PO_3 denuders are working optimally. When denuder scrubbing efficacy was found to be not optimal (<95%), this indicates that replacement with newly coated denuders is required, simultaneously flagging the portion of the dataset where acidic or basic measurements may be biased or compromised. The gaseous NH_3 calibration source, generated using a permeation device (PD) and thermostated oven, was used to ensure the conversion efficiency of the Pt catalyst in the tN_r oven was quantitative and not degrading over time. High mixing ratios of NH_3 were used to ensure 100% conversion was observed, as quantitative conversion below this level could then be readily assumed. We set this upper limit at 200 ppbv for NH_3 based on prior reports in the literature indicating that this mixing ratio is near the upper limit of the range typically found in indoor environments[19]. Furthermore, NH_3 can

be used to check the tN_r oven performance over time, as its conversion to NO_x will be the first to reflect any degradation in catalytic efficacy.

The HONO calibration source has been described in detail by Lao et al.[45]. Briefly, the HONO calibration source generates HONO mixing ratios in the low ppbv range via an acid displacement reaction (R1). Gas-phase HONO is generated by passing dry zero air over a HCl PD to combine with an equal flow of air saturated with water vapour, which then enters $NaNO_2$-coated reaction devices at a total flow of ~110 ccm and 50 % relative humidity (RH). In this work, HONO mixing ratios of up to 20 ppbv in a flow of 1 litre per minute (lpm) of zero air were generated by inserting a custom-made HCl PD (12 M HCl in 1/8-inch OD tubing of 8.5 cm in length) and two $NaNO_2$ reaction devices connected in series. These were housed in an oven set to 40 °C. Impurities of NO were below detection limits (0.43 ±0.49 ppbv) during the experiments.

$$HCl_{(g)} + NaNO_{2(s)} \rightarrow HONO_{(g)} + NaCl_{(s)} \qquad (R1)$$

Similarly, dry zero air was passed over a PD containing NH_4OH (30% v/v in 1/8-inch OD tubing of 9 cm) to produce gas-phase NH_3. The output and stability of this PD was confirmed by regular scrubbing in to 1 mM HCl followed by Ion Chromatography (IC) measurements by conductivity[55]. The output mixing ratio was determined to be 3 ppmv in a flow of 90 ccm. Prior to addition to the instrument inlet, the NH_3 PD output was diluted with zero air (4-5 lpm), to generate NH_3 mixing ratios on the order of 30 ppbv.

2.1.6 Instrument control and data acquisition (DAQ)

Automated control of the solenoid valves and mass flow controllers (Fig. 1) was achieved using a DAQ device (T7 and PS12DC, LabJack, Lakewood, CO, USA) and a custom-built LabView program (National Instruments). Full details and electronic schematic diagrams of the instrument control system are available in the SI (Section S2, Fig S3). The LabView program VI can be found on the tNr instrument GitHub repository[56], with further information in Section S2. Briefly, the LabView program allowed for the individual solenoid valves to be switched on separate time intervals as required, with input variables easily adjustable (e.g. valve timings, flow rates). Measurements of NO_x from the Serinus 40 were recorded via the analog output channels (NO, NO_2 and NO_x) using the DAQ at a one second time interval. The LabVIEW program controlled and recorded the valve actuations, MFC flow rates, and NO_x readings (converted to ppbv based on a determined analyser transfer function from the analog voltage output). These values were stored in one text file for post- processing, as described in the next section.

2.1.7 Data Analysis

The tN_r instrument LabVIEW program generated a data file that was processed using custom R script in R studio (v3.6.1) available on our Github repository[56] (SI, Section S3). Briefly, the data processing script first organized the tN_r dataset by separating data collected in each sampling pathway, and then averaging all the measurement data to a one minute time interval, matching the response time of the NO_x analyser (see below). The first minute of each measurement cycle (e.g. NO_x, $N_{r,acid}$, tN_r or $N_{r,base}$) was removed to avoid any bias from transfer delays or pressure-induced measurement fluctuations related to valve changes. Each measurement cycle is continuous for 5 minutes and takes place every 20 minutes. Between these measurements, we applied a linear interpolation to estimate the intervening 15 minutes of data. The primary motivation for this was to facilitate continuous calculation of the acidic and basic N_r fractions. We acknowledge that using a linear interpolation assumes the rate of change in analyte levels is either unchanged or slowly linear compared to the period between each measurement cycle. This is generally

true for the majority of measurements of our target analytes made in indoor environments with low air change rates (e.g.[27,46,57]) but may result in an overestimate or underestimate bias during periods of rapid changes in ventilation or emissions, respectively. Consequently, final validation of any collected datasets requires detailed inspection of the interpolated data to identify periods when the tN_r (or a particular species within it) is changing in concentration faster than the duty cycle time of 20 minutes. During such periods, all measured data were kept, but interpolated data were removed to prevent systematic bias.

2.2 Instrument Validation Experiments

2.2.1 Response time – positive and negative control experiments

To build an accurate and real-time gas detection platform, we must understand the instrument response time to changes between sampling pathways, concentration, and flow rate when handling a sample that is representative of the indoor atmospheric matrix. Therefore, a series of control experiments were designed to characterise the instrument response time to changes in mixing ratios of key N_r for the different instrument settings, e.g. between NO_x and $tN_{r,gas}$ measurements. For these experiments, the instrument inlet was overflowed with dry zero air, followed by sampling a flow of an N_r species of interest at a known mixing ratio by switching a valve. Once a stable mixing ratio through the instrument was achieved, the N_r species was removed from the flow, and the decay in mixing ratio was recorded until it reached background levels observed when measuring zero air. The experiment was done for NO_x and the tN_r pathways for NO, NO_2, and HONO. With respect to the tN_r oven, NH_3 and five selected alkyl amines that are commonly abundant in indoor air were also tested. The response time for the Na_2CO_3 and H_3PO_3 denuders to scrub HONO and NH_3, MMA and DEA, respectively were also tested using a similar experimental set up.

All measurements for the time response experiments used one second measurements from the analog voltage output from the NO_x analyser, converted to a mixing ratio in ppbv, and averaged to a 12 s time resolution (equivalent to the sample cycle interval of the analyser). The time response was calculated according to Moravek et al.[58], by single exponential fit of the decay to background from a stable mixing ratio (Eqn 4) to calculate the time constant, τ, for all experiments.

$$f(t) = y_0 + A \cdot exp\left(\frac{-(t-t_0)}{\tau}\right) \qquad \text{(E4)}$$

The time response was calculated to 98% (i.e 4τ). For more inert species where wall interactions are not important (e.g. NO_x), E4 should accurately represent the instrument time response. For more reactive or surface-interacting species, such as NH_3, where wall interactions are expected to be significant, a double exponential fit of the decay to background was calculated when beginning from a stable mixing ratio according to Eqn 5 [58].

$$f(t) = y_0 + A_1 \cdot exp\left(\frac{-(t-t_0)}{\tau_1}\right) + A_2 \cdot exp\left(\frac{-(t-t_0)}{\tau_2}\right) \qquad \text{(E5)}$$

Where y_0 represents the measured instrument baseline level, A_1 and A_2 are the proportionality coefficients for the physical processes of sample volume exchange in the inlet and reaction cell, and wall interactions, respectively. The values of τ_1 and τ_2 are the time response of the two respective processes. The start time for the removal of the analyte from the flow of zero air is denoted by t_0. The percentage contribution of the wall interaction process can be described by the term D (E6) [59]

$$D = \left(\frac{A_2}{A_1 + A_2}\right) \times 100\ \% \qquad \text{(E6)}$$

Along with τ_1 and τ_2, D can be used to evaluate the extent of surface processes in governing the time response of the tN_r instrument with respect to different N_r species.

2.2.2 Conversion efficiency of total Nr Oven

Quantitative measurement of the tN_r budget requires near unity conversion of even the most challenging of N_r species to NO_x in the instrument. Therefore, the conversion efficiency of the total N_r oven was determined by adding known amounts of select N_r species, that span a wide range of N bond energies, and ensuring the NO_x conversion requirement was met. Mixtures of NO_2 in zero air that spanned typical indoor levels (20-130 ppbv) were generated using the gas calibration system and corresponding standard cylinders. A standard mixture of HONO in zero air was generated using the integrated calibration source described above (Section 2.1.5). The output NO, NO_2 and HONO mixing ratios were verified by measurement with the NO_x analyser prior to addition to the oven.

Fully reduced N_r species are particularly challenging to convert to NO_x, so NH_3 and several amine standard mixtures were made using a custom-made PD installed in the integrated calibration source (Section 2.1.5). For the amines, PDs of MMA (40% w/w), DMA (40% w/w), DEA (≥ 99.5% w/w) and TMA (45% w/w) solutions were made similarly to NH_3. During the experiments, each PD was heated to 40 °C under a constant flow of zero air (ca. 50 ccm), which was diluted further with zero air to achieve a desired mixing ratio. All flowrates in these experiments were verified with a bubble flowmeter (Gilibrator-2, Sensidyne®) when calculating dilution factors. The outputs of the NH_3 and each of the amine PDs were determined by quantitation using our established IC method[55] prior to the experiments. We also varied the flow rate through the instrument inlet from 0.63 to 2.0 lpm using an additional MFC to change analyte residence times to quantify any effects on CE in the tN_r oven for NO_2, HONO and NH_3.

3.0 Instrument characterization and validation

3.1 Instrument response time

The response times in the NO_x and tN_r pathways were determined experimentally, as detailed in Section 2.2.1 and the results are summarized in Tables 2 and 3. For NO, NO_2, and HONO the response times (4τ) were found to be similar at approximately 1 min when sampling with an instrument inlet flow of 630 ccm (Table 2). The response times calculated from these experiments used a single exponential fit (98 – 0 %). A comparison of single and double exponential fits was also made (Table S1), but this analysis found that both τ values were similar. This result indicates that the D value, representing wall interactions of NO, NO_2, and HONO were all similar. The response time experiments were repeated at different flow rates through the NO_x sampling pathway for NO and NO_2 and response time was found to be independent of the instrument inlet flow rate from 630-2000 ccm (Fig S5, slopes of -2.99×10^{-4} and 4.67×10^{-5} $min^2\ cm^{-3}$, respectively). For HONO the response time was also independent of instrument flow rate through the NO_x and tN_r sampling pathways (Figs S5 and S6, slopes of $-3.79 \times 10^{-4} \pm 5.93 \times 10^{-4}$ and $-6.55 \times 10^{-5} \pm 2 \times 10^{-4}$ $min^2\ cm^{-3}$, respectively) and in the NO_x sampling pathway (Fig S4). In each case, there are no linear trends as all calculated regression slopes were within a value of zero when considering the uncertainties (1σ).

All three compounds demonstrating the same ≤1 min response times indicating that the instrument was only constrained by the sum of the rate of inlet air exchange and that of the NO_x analyser, inclusive of the instrument response time. Since the increased instrument inlet flow had no effect on NO, NO_2, and HONO response times, it indicates that these species are not substantially adsorbing onto the PFA inlet surfaces, as we have previously reported for other HONO sampling strategies[60]. Similarly, transfer of higher mixing ratios of HONO did not increase the response time, demonstrating that there was no adsorptive buildup of HONO on surfaces in the instrument inlet lines, making the response independent of HONO mixing ratio.

Table 2. Average (n=3) response time (98-0%) at a flow rate of 630 ccm through the two sampling pathways of the tN_r instrument calculated by a single exponential fit. Variability shown is one standard deviation from the mean.

	NO_x Pathway		**tN_r Pathway**	
N_r species	*Response time (4τ, mins)*	*Mixing ratio (ppbv)*	*Response time (4τ, mins)*	*Mixing ratio (ppbv)*
NO	1.1 ± 0.1	17.9 ± 0.8	0.9 ± 0.1	18.4 ± 0.6
NO_2	0.5 ± 0.1	17.6 ± 1.1	0.7 ± 0.1	23.0 ± 0.5
HONO	1.0 ± 0.1	20.2 ± 1.1	0.9 ± 0.1	13.1 ± 2.1

The response time (4τ) for NH_3 in the tN_r pathway calculated using E4 was 5.5 mins, while for amines it ranged from 13-24 mins, which are notably longer than those calculated for NO_x and HONO. This likely reflects the fact that wall interactions led to increased response time with respect to NH_3 and amines (e.g.[58] and references therein). We therefore applied E5 and E6 to separate the role of the volume exchange and wall interaction processes to determine the overall instrument response time for this basic compound class (Table 3, with representative normalised decays shown in Fig S7). For NH_3 and amines, τ_1 was calculated to be 29-62 s (Table 3), higher than that calculated for NO_x and HONO (Table 2; 4τ of 0.7-0.9 min, equivalent to τ of 11- 14 s) and the calculated turn over time of 2.6 s based on the internal tubing volume of the instrument inlet (27.7 cm^3). The calculated τ_2, which is representative of the effect of wall interactions on NH_3 and amine, varied considerably, but was about an order of magnitude larger ranging from 221-639 s. The longer response time for the instrument to NH_3 and amines were expected as they undergo strong inter-molecule interactions with any interfacial water on tubing surfaces and may also partition into its polymeric matrix before the tN_r oven. This behaviour is analogous to the gas-wall interactions for semi-volatile organic compounds, which are known to exhibit absorptive partitioning behaviour on PFA tubing, resulting in measurement delays[61,62]. NH_3 was found to have a lower τ_2 compared to the tested amines (Table 3), indicating it was less affected by wall interactions. From Fig S7, NH_3 reached zero faster than amines (which all displayed similar normalised decay) and after 5 mins was within 20-30% of the maximum level before delivering zero air.

Table 3. Calculated response time (98-0%) through total N_r sampling pathway for basic N_r species at flowrate of 630 ccm fitted by a double exponential fit. Variability shown for the input mixing ratio is one standard deviation of the mean, while for τ_1 and τ_2 it is the standard deviation of the fit.

Basic N_r species	**Input mixing ratio (ppbv)**	**τ_1 (s)**	**τ_2 (s)**	**D (%)**
NH_3	24 ± 1	29 ± 6	220 ± 60	41%
MMA	23 ± 1	30 ± 4	640 ± 60	46%

DMA	26 ± 1	55 ± 5	610 ± 70	36%
DEA	25 ± 1	62 ± 9	380 ± 40	45%
TMA	6 ± 1	40 ± 30	450 ± 200	52%

It should be kept in mind that during field measurements ambient NH_3 levels are not likely to go to zero after sampling a source of high emissions. Therefore, the response times presented in Table 3 are not representative of performance under normal operation in nearly any indoor environment. A more realistic experiment for determining the instrument response time is to add a pulse of NH_3 to ambient air and measure the decay back to ambient levels (i.e., a standard addition approach). This experiment was performed by adding pulses of NH_3 at two mixing ratios, 30 ppbv (n=3) and 200 ppbv (n=2) to ambient laboratory air and monitoring the normalised decay back to background levels (3-6 ppbv) as shown in Fig 2. Time for the instrument to reach background levels of NH_3 were found to be similar for both additions. The instrument response time in these experiments had τ_1 and τ_2 calculated to be on average (±1σ) 20 ± 8 and 270 ± 150 s, with a D of 24 ± 15%. The calculated time response to reach background levels of NH_3 (Fig 2) resulted in a lower τ_1 and D (Table 3) but a similar τ_2 compared to the experiments performed with zero air. The lower D value indicates that wall interactions reduced in relative importance during the standard additions experiment (Fig 2). This would contribute to the instrument τ_1 improving from 29 ± 6 to 20 ± 8 s when using the more representative approach to indoor sampling.

Overall, the results in Fig 2 and Table 3 demonstrate that the instrument is able to capture temporal trends in NH_3 and amines if ambient levels are changing at timescales on the order of a few minutes. This is likely to be the case in indoor air as it is typically well mixed. Perturbations in moderately lived species like NH_3 are observed from direct sources (e.g. cooking, cleaning), modulations in ventilation system operation, or opening and closing windows and doors.[19,40] Where such conditions cause rapid sub-minute changes in these compounds, this instrument may not capture the true temporal variability, but instead exhibit a small time lag with lower peak mixing ratios measured.

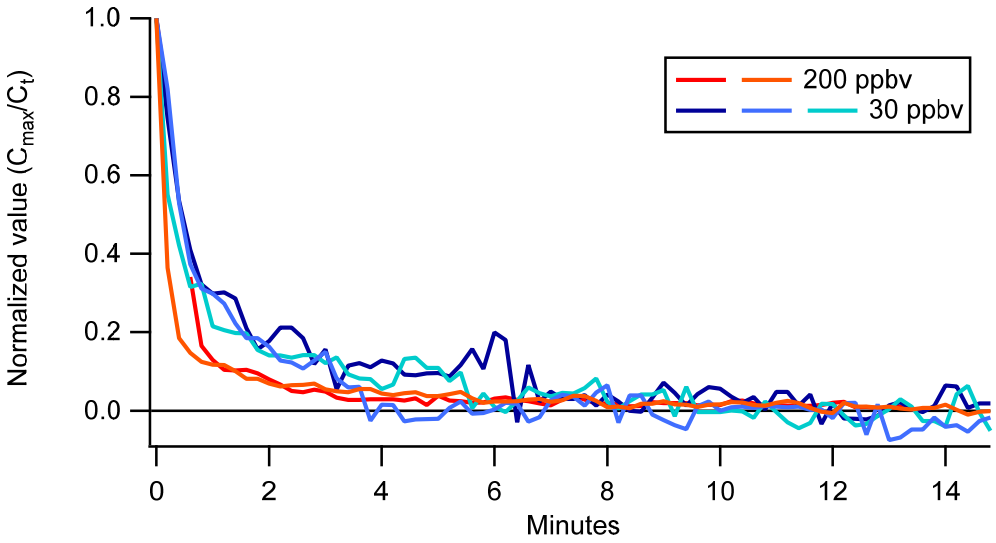

Fig 2. Normalized decay of NH_3 pulse to background ambient levels during standard additions to the inlet. Red traces denote duplicate experiments with 200 ppbv of NH_3 added, while blue traces denote the triplicate experiments with 30 ppbv additions.

3.2 Response time and scrubbing efficacy of denuders

In order to enable measurement by difference for the target species HONO and NH_3 by the Na_2CO_3 and H_3PO_3 denuders, respectively, we must scrub these species fast with a high efficacy. The utilised denuders are designed for this task and were validated experimentally (Table 4). The response time to scrub HONO by the denuder was calculated to be 1 min. As with the instrument response time for NO, NO_2, and HONO, the denuder response time is limited by the response of the inlet air exchange rate and NO_x analyser detector. The scrubbing efficiencies of HONO were determined at two relevant mixing ratios for indoor air: 14 ppbv and 4 ppbv, with the fraction captured observed to be greater than 99.6% (Fig S8).

The H_3PO_3 denuder was also confirmed to be effective at scrubbing NH_3 and selected amines (MMA and DEA) in the ppbv range with the fraction captured greater than 99% (Table 4). The response time using normalized decay for scrubbing NH_3 and selected amines with the H_3PO_3 denuder was calculated by E5 (Fig S9). For NH_3, τ_1 and τ_2 were 14 ± 2 s and 170 ± 110 s (1σ), respectively, with a D value of 12%. For DEA, τ_1 and τ_2 were 27 ± 3 s and 240 ± 370 s (1σ), respectively, with a D value of 6%. The low D value indicates that sample volume exchange was the dominant process for NH_3 and DEA, which makes sense given the small remaining inlet volume between the exit of the annular denuder and the catalytic furnace in these experiments. From Fig S9, within 2 mins the measured levels were below 10% of the known input levels for both NH_3 and DEA. Overall, the results of these experiments demonstrate that denuders were effective at scrubbing the targeted atmospheric bases fast enough to enable measurement by difference on timescales of a few minutes.

A stable mixture of NO and NO_2 (18 ± 1 ppbv and 17 ± 1 ppbv, respectively) was sent through the Na_2CO_3 denuder to ensure that no significant adsorption or chemical loss of NO_x occurs on the surfaces of the denuder or its coating. There was no decrease in NO levels observed when it transited the denuder compared to bypassing the denuder (Fig S9). The same experiment was carried out with NO_2 (Fig S10) however a small decrease of NO_2 of 0.3 ± 1.6 ppbv lost to the denuder was observed. The same experiment was carried out with NO_2 (Fig S11) however a small decrease of NO_2 of 0.3 ± 1.6 ppbv lost to the denuder was observed. The measured levels of NO_2 bypassing and transiting the denuder were compared using a two-tailed t-test and were found to not be statistically different at a 95% confidence interval ($p = 0.13$). This means that there was a measurable but insignificant loss of at most 2% of NO_2 when passing through the denuder, possibly due to chemical loss to the coating and/or surface of the denuder. Previous studies have observed loss of NO_2 to carbonate denuders[46,63]. Zhou et al.[46] reported an average decrease of 2.6 % NO_2 after flowing 13 to 270 ppbv into a denuder, which is similar to the upper limit of our findings. The 2% loss of NO_2 to the denuder will be considered as a worst-case outcome when quantifying the mixing ratio of HONO, resulting in a conservative estimate. These experiments give confidence that the instrument measurements are capable of quantifying of indoor mixing ratios of NO, NO_2, and HONO.

A very small positive bias due to HONO formation in the sampling line was found when it was experimentally exposed to a mixture of humid air representing indoor conditions (42-50% RH) and NO_2 (24-305 ppbv), resulting in an average conversion of 0.8% (Fig S12/Table S2). Mixing ratios of NO_2 up to 300 ppbv were tested to be representative of the upper limit for the range typically observed indoors,

originating from combustion processes like cooking with a gas stove [46,64–66]. All of the components used in the tN_r instrument inlet (i.e. valves, fittings, tubing) were made of PFA as it is one of the most chemically inert materials in comparison to others available, such as glass inlets, that can result in a strong production of positive artifacts[67]. The observed loss of NO_2 to the Na_2CO_3 coating (2%) would have included heterogenous HONO formation by NO_2 hydrolysis on the sampling lines upstream. For example, if levels HONO and NO_2 were 2 and 20 ppb, the additional 0.4 ppbv loss of NO_2 on the denuder would propagate to a relative error for HONO of 0.85 ppbv**.** Overall, up to 2% of NO_2 can potentially be lost within the sampling line by the surface reaction of NO_2 under typical indoor RH conditions, and these observed losses were just as probable to have been driven by instrument drift and/or noise so the example relative error estimate for HONO represents a conservative upper limit**.** These negative in NO_2 and positive in HONO biases were not corrected in our proof-of-concept work presented in Section 4 as the potential artefact is typically within the precision of the instrument.

Table 4. Calculated response time (4τ) and scrubbing efficacy of carbonate (HONO) and H_3PO_3 (NH_3) denuders at a flow rate of 630 ccm. Response time reported for NH_3 and amines using τ_1. Where indicated N/A means a particular test was not possible. Variability values provided are one standard deviation from the mean when replicates were conducted.

	Response time (4τ, min)	Input mixing ratio (ppbv)	After denuder (ppbv)	Fraction captured (%)
NO_x – HONO (n=3)	1.0 ± 0.2	14 ± 1.0	0.1 ± 0.7	99.6
NO_x – HONO (n=4)	1.0 ± 0.4	4 ± 1	-0.6 ± 0.6	115
NO (n=3)	N/A	18 ± 1	18 ± 1	0.0
NO_2 (n=3)	N/A	17.3 ± -1.1	17.0 ± 1.2	2.0
tN_r – NH_3 (n=3)	0.9 ±0.1	25 ± 1	-0.1 ± 0.4	100.4
tN_r – MMA (n=1)	3.0	10 ± 1	-0.3 ± 0.3	103
tN_r – DEA (n=1)	1.8	35 ± 1	0.1 ± 0.3	99.7

3.3 Conversion efficiency of reactive nitrogen species in the tN_r oven

For quantitative measurement of the total N_r budget, the tN_r oven must efficiently convert N_r species to NO_x. The conversion efficiency (CE) to NO_x for key N_r species (HONO, NH_3 and selected amines) found indoors was determined experimentally. Overall, the observed CE of these species was 100% within measurement uncertainty (Table 5) at a flowrate of 630 ccm and tN_r oven temperature of 800°C. The CE of NH_3 was consistently observed to be above 100% (103 ± 24%, Table 5), an observation also reported by Stockwell et al.[31] MMA had the lowest CE (80 ± 21%), while the other tested amines ranged from 88 to 106%, which may indicate a potential to underestimate the total amount of amines. Note that all were within 100% CE, when propagating the uncertainty determined by the IC quantitation and NO_x analyser detection schemes. A small fraction of the NO_x generated by the catalytic oven when converting these analytes was observed as NO_2 at 800 °C (<6%), indicating that the oven was efficient at converting each species to NO, and suggests that limited back reactions occurred to form NO_2 [31,68]. The

CE for NO_2 was determined to be independent of flowrate between 630-1500 ccm (Fig S13). While for NH_3, CE decreased with increasing flowrate (Fig S14). This makes sense as fewer collisions with the hot Pt will occur due to decreased residence time over the catalytic surface in the oven. The observed CE in the current work is comparable to previous reports (Table 5). Overall, our assessment validates that efficient conversion of key nitrogen species was achieved, but some additional considerations regarding temperature characterization for these systems was realized.

Table 5. Experimentally determined conversion efficacy (CE) for key species through tN_r oven at 800 °C in nitrogen (0% RH) with a flow rate of 630 ccm. Also shown as a comparator is the reported CE to NO_x under similar conditions by Stockwell et al.[31] Variability presented for CE is a propagation of measurement uncertainty (1σ) while for input mixing ratios it is one standard deviation of the mean output.

Species	CE to NO_x	Input mixing ratios (ppbv)	CE reported by Stockwell et al.[31]
NO_2	98-100%	20-130	99 ± 2%
HONO (n=3)	99 ± 3%	13 ± 1	Not reported
NH_3 (n=3)	103 ± 24%	30 ± 1	105-110 ± 15%
NH_3 (n=2)	109 ± 24%	194 ± 2	
MMA (n=1)	80 ± 21%	23 ± 1	95 ± 15%, triethyl amine (TEA)
MEA (n=1)	101 ± 17%	12 ± 1	
DEA (n=1)	88 ± 32%	25 ± 1	
DMA (n=1)	106 ± 24%	26 ± 1	
TMA (n=1)	97 ± 16%	6.2 ± 0.7	

3.3.1 Effect of temperature on reduced nitrogen species conversion to NOx

The most important factor that controlled the conversion efficiency of NH_3 and tested amines was the tN_r oven temperature. Previous work by Stockwell et al. [31] observed quantitative conversion of NH_3 on Pt catalyst heated to 750°C, similar to commercial instruments (e.g. Thermo 17i) but cooler than that used in the current work. Fig 3 shows that CE for NH_3 and selected amines underwent a rapid increase in the fraction converted between 600-700°C. For NH_3, the CE increased from 70% at 600°C to 100% at 700°C. A similar pattern in the CE of DMA and TMA were also observed (Fig 3). The exception was MMA, with the CE only increasing minimally between 600-900°C (<10%, Fig 3). This sharp effect from temperature on catalyst performance has been shown previously for NH_3 on a heated molybdenum oxide (MoOx) catalyst[69] and is expected for any catalytic system where the temperature determines whether the altered activation energy of the surface-mediated decomposition pathway is exceeded. Since a large and rapid decrease in CE can occur over a narrow temperature range (roughly 75°C or 11-13% of the oven temperature), this indicates that accurate and regular characterization of conversion requires a stable oven temperature and precise temperature control to ensure optimal conversion of reduced nitrogen species.

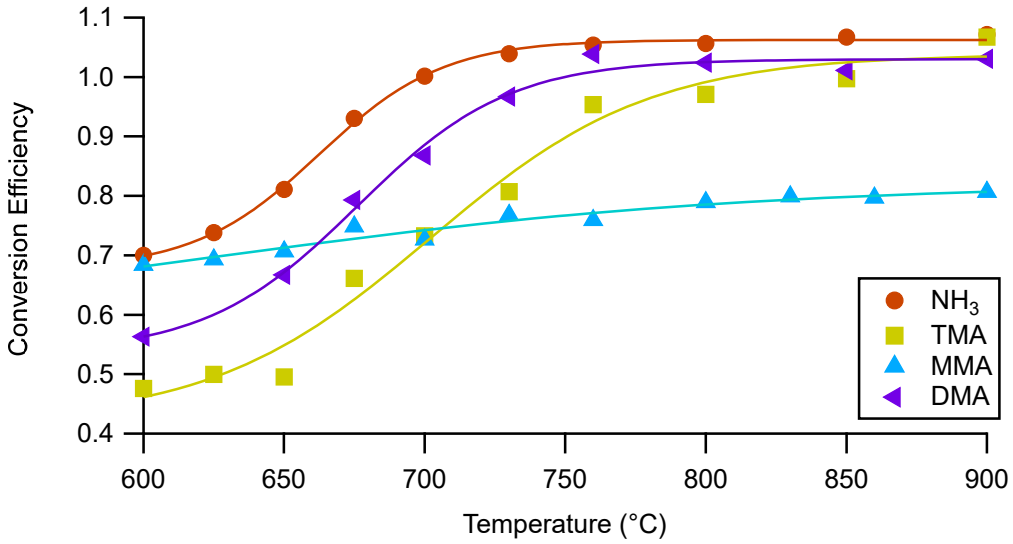

Fig 3. Conversion efficiency for NH_3 (25 ppbv), MMA (23 ppbv), DMA (26 ppbv) and TMA (6 ppbv) to NO_x in the tN_r oven as function of temperature at a flow rate of 630 ccm. A sigmoid curve has been drawn through each species. The measurement variability for the conversion efficiency of each species was given in Table 5.

4.0 Proof-of-concept field measurements in a commercial kitchen

Proof-of-concept measurements with the tN_r instrument were performed in a commercial kitchen on a university campus in Toronto. An in-depth analysis of measured tN_r species and budget is outside the scope of this work. In the current work, we present a time series of measured tN_r budget from days with high and low levels of cooking activity to validate the capabilities of the tN_r instrument when sampling a highly dynamic and complex gas mixture that was encountered in this indoor environment.

4.1 tN_r Instrument set up and field quality control procedures

The tN_r instrument was housed inside an air-conditioned room, with the inlet line sampling from the main cooking area (¼ inch OD PFA tubing, 6.6 m long, total flow of 2.1 lpm). Equipment near the inlet included ovens, gas stoves, and dishwashers. The kitchen volume was approximately 620 m^3 with a calculated geometric surface area of 1970 m^2. A PTFE filter was installed at the inlet to remove airborne particles. For these measurements the tN_r instrument was set to sample for 5 min per pathway (NO_x^*, NO_x, $tN_{r,gas}$ and $tNr_{scrubbed}$, Table 1 and Figure 1) for a total duty time of 20 mins. The instrument flowrate was set to 630 ccm during the measurements, to yield the maximum conversion efficiency found from our characterization tests. The operating temperature of the tN_r oven was set to 800°C. The NO_x analyser was calibrated with a gas-calibration instrument and a standard gas cylinder of NO (5 ppmv in N_2) prior to the measurements as per manufacturers specifications. A second chemiluminescent NO_x analyser (Ecotech EC9841) also sampled from the sampling line during the campaign to give independent measurements of NO_x at one minute time resolution. This analyser was calibrated using the same procedure as the tN_r instrument NO_x analyser. The measured NO, NO_2* and NO_x* from the tN_r instrument agreed well with the EC9841 over the campaign, with slopes of 1.0, 0.96 and 1.0, respectively (r^2 = 0.96). The excellent agreement between the NO_x measurements indicates that the tN_r instrument inlet was not affecting the measured NO_x.

During the measurements, regular quality control checks were performed using the in-situ zero air and calibration sources during periods when low activity was observed in the kitchen (see Table S3 for typical order of operations). Field blank measurements for the NO_x and tN_r sampling pathways were performed by overflowing the instrument with zero air. No drift in the zero measurement was observed on the NO_x sampling pathway, with precision of 0.53 ppbv. This was not the case when zero air was passed through the tN_r oven, where a high baseline (ca. 4 ppbv of NO_x) was observed after 15 mins of exposure to zero air. Extended flushing of the oven with zero air was found to reduce the NO_x output of the tN_r oven to less than 1 ppbv of NO_x, consistent with observations when delivering dry compressed zero air from cylinders. We suspect the contamination observed in the zero-air overflow of the oven was due to recalcitrant tN_r fraction 'poisoning' the Pt catalyst, which is well known for Pt and reduced nitrogen in organic synthesis. In this commercial kitchen, ammonia and amine levels were unexpectedly high – on the order of tens of ppbv. As a result, we implemented a regular system check where the tN_r oven was regularly cleaned (ca. every 2 days for 30-120 min, Table S3) with zero air until the measured tN_r reached was equivalent to that observed when zero air bypassed the oven and was delivered directly to the NO_x analyser (i.e. <1ppbv NO_x). Permeation devices for HONO and NH_3 were installed in the permeation oven to assess the scrubbing efficacy of the Na_2CO_3 and H_3PO_3 denuders, respectively. Both denuders were exchanged every two days with freshly coated replacements. Prior to exchanging, the installed denuders were tested for their scrubbing efficacy. During this pilot study, we always observed this property to be greater than 95%. Similarly, the freshly prepared and installed denuders had their scrubbing efficacy confirmed prior to use. Taken together, these quality control checks contribute to the assertion that the acidic and basic fraction measurements are quantitative.

To conclude that measurements were complete and quantitative, NH_3 was also used to assess the conversion efficiency of the tN_r oven in-situ during the measurements. During the campaign, the CE was observed to range between 70 to 130%, with a mean of 110%, comparable to the values and range observed during laboratory testing (Table 5). The observed variance is driven by the known variability in the NH_3 PD output[70] (±30%) and, as a result, can only be used semi-quantitatively when assessing changes in Pt catalyst conversion efficiency over time. Consequently, we did not apply a correction factor for NH_3 conversion in the oven due to this observed variability in the NH_3 source, but this could be done in the future if a more stable source of NH_3 is used, such as a calibrated cylinder[71,72]. During the measurement period, Ogawa passive samplers with citric acid-coated reactive substrates were installed in the kitchen close to the sampling inlet for an intercomparison of measured gas-phase NH_3 and amines levels. The passive samplers were deployed for two periods, 7-13 and 13-17 Sept, and were extracted in milli-Q water followed by analysis by IC-CD, with full details available in Salehpoor et al[55]. The measured levels of NH_3 and amines by passive sampler were used as a further quality check on the tN_r performance and are presented in the following section.

4.2 Time series of measured tN_r and species in a commercial kitchen

The tN_r instrument measured for 12 days continuously in the kitchen without any instrument faults. Data capture across these days was high (86%). Time series of measured tN_r and NO_x levels, along with calculated HONO and basic N_r for selected days with high and low cooking activity demonstrate the high data capture (Fig 4), with measurement gaps (<2 hrs) corresponding to calibration or other quality control checks (Table S3). Levels of tN_r were fairly consistent over these 2 days, with sharp peaks observed during reported cooking times (e.g. 10 am – 12 pm on 15 Sept). Outside these times, in the afternoon and at night, stable levels of tN_r were observed (Fig 4). The apparent varying readings in tN_r

and $N_{r,base}$ during these periods reflects linear interpolation between measurements for these fractions, but are within the propagated error estimates of 20% in our CE estimates. Furthermore, the excellent agreement in the time trends between the measured NO_2 for both instruments indicates that tN_r is capturing the temporal trends. On 11 Sept no substantial peaks in tN_r were observed, as there was limited cooking in the kitchen on this day. The measured tN_r reached over 100 ppbv during cooking periods and were typically driven by NO_x. Previous work has observed levels of NO_x, HONO and NH_3 greater than 100 ppbv during cooking in domestic settings[18,19]. The observed sharp peaks in tN_r result from rapid intense cooking emissions coupled with very high ventilation rates in the kitchen (average daytime air exchange rates were 27 ± 7 h^{-1}). Unfortunately, HONO or basic N_r fraction levels in the cooking plumes could not be calculated (Section 2.1.7) reliably during such times, as the N_r was changing faster than the instrument duty cycle (20 mins). Consequently, the instrument was challenged to measure short peaks in HONO or basic N_r in the kitchen that were fully ventilated in 20 minutes or less. Such high ventilation rates driving very rapid changes in NO_x is atypical for indoor environments[57] and this instrument was designed to be capable of quantitatively capturing dynamics in these more limited ventilation environments. For example, the commercial kitchen measurements at night demonstrate that the tN_r instrument can reliably measure the tN_r budget, and longer-lived oscillations readily.

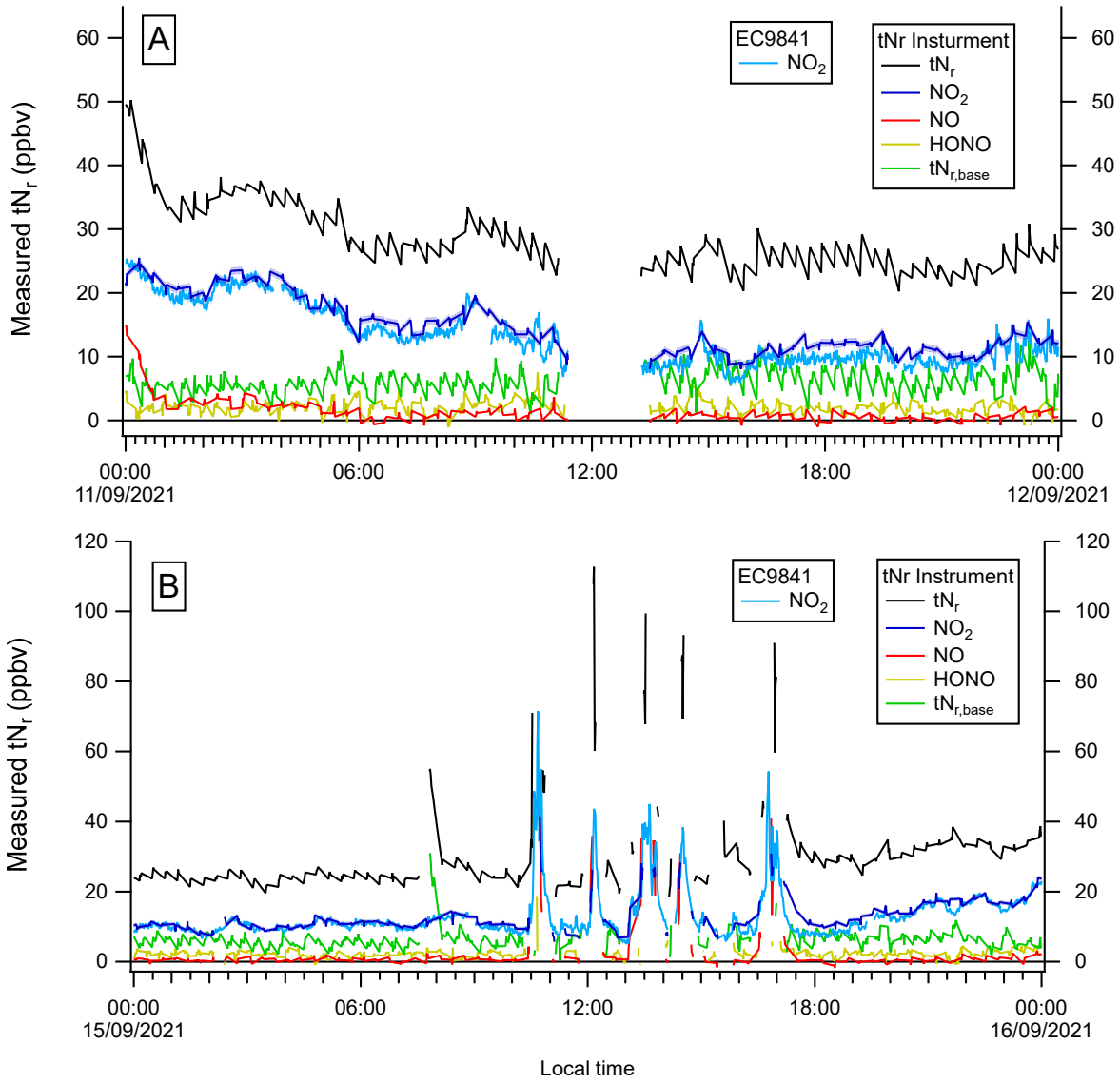

595

Fig 4. Selected days of one minute time resolution tN_r measured and speciated with interpolation between measurement periods for a) low cooking day (11th September) and b) high cooking day (15th September). Gaps across all measurements are due to instrument quality control activities, while those isolated for HONO or $N_{r,base}$ result from periods where emission peaks are shorter lived than the
600 instrument duty cycle. Also included are measured NO_2 levels by co-located EC9841 NOx analyser for comparison, with the shaded areas indicating the measurement uncertainty. Note the different y axis scales.

The majority of the measured tN_r was NO_2 in the kitchen (43%, Fig 4), followed by the $N_{r,base}$ fraction (23%). The basic fraction is likely comprised primarily of NH_3, whose sources would include cooking,
605 cleaning, and human emissions, all expected to be present with significant frequency in a kitchen[19,20] . Amines would also be measured in this fraction, which have similar sources (e.g. cleaning and cooking[21,25,26]), so these are expected to contribute to the observation although they cannot be speciated by this measurement approach. The measured levels of NH_3 from the passive samplers were

found to be comparable to average $N_{r,base}$ measured by the tN_r instrument over the same time period (Fig S15). The agreement with the passive sampler results provides an orthogonal assessment that the measured levels of the $N_{r,base}$ fraction by the tN_r instrument are reliable and accurate. They also indicate that NH_3 was the major contributor to $N_{r,base}$ since detectable levels of alkyl amines were not identified in the passive sampler extracts. Overall, it was expected that the basic N_r fraction measured by the tN_r should be equal or higher than the measured NH_3 by passive sampler, but a possible driver of the slight mismatch with passive quantities being higher is that the tN_r instrument dataset would miss short, sharp peaks in NH_3 during direct emission events. Extraction and analysis of the annular denuder on this flow pathway could provide its own time-integrated compositional view, provided it has not been exposed to NH_3 for scrubbing calibration gas or conversion efficiency checks, which was the case here. The relatively high contributions from $N_{r,base}$ likely reflects the prevalence of cooking and cleaning in a commercial kitchen. The proportion of other tN_r species was also fairly consistent outside of cooking times, with the exception of NO. Higher levels of NO were observed during the early morning before the kitchen opened (5-8 am) were likely due to the intrusion of polluted outdoor air. Overall, the tN_r budget was not closed by measured NO, NO_2, HONO and $N_{r,base}$ species. The 'missing' fraction was stable throughout the day, at around 5 ppbv or 18% of the measured tN_r. As acidic and basic N_r species would be measured by the tN_r instrument (Table 1), neutral N_r species most likely comprised the missing fraction, and identifying the species in the missing fraction will be the focus of future work.

5.0 Instrument application for indoor air chemistry

Here we have described an instrument for measuring the tN_r budget and key species NO_x, HONO and basic N_r in indoor environments. The measurement approach was validated through a series of controlled experiments, and quantitative measurement and speciation of the tN_r budget was demonstrated. The optimum operating conditions of the tNr oven were found to be 800°C with a sampling flow rate of 630 ccm, which also yielded an acceptable time response for NO_x, HONO, NH_3 and relevant amines of importance indoors. The efficiency of the tN_r oven to convert reduced N_r species to NO_x reached a maximum at 800 °C, at 103 ± 13% for NH_3 and 79-106% for the tested amines, demonstrating the importance of conversion temperature characterization for the tN_r oven. The tN_r instrument was successfully deployed in a commercial kitchen, a complex indoor environment with periods of rapidly changing levels and shown to be able to reliably measure the tN_r budget during period of longer-lived oscillations (>20 mins), more typical of most indoor spaces.

Recent work has shown how humans significantly affect the chemistry of indoor air [20,41,73], illustrating the importance of surveying occupied spaces to fully understand indoor air quality and occupant exposure to pollutants. Therefore, unobtrusive measurements, to avoid affecting occupants and influencing their activity during measurements, are paramount to understanding what people are exposed to indoors. Yet an instrument package with sufficiently high time resolution is required to fully probe chemistry involving a multitude of species in indoor air and the complex interplay between chemistry, ventilation and surfaces[53,74], perhaps best illustrated by the HOMEChem study[27]. While this prior study allowed researchers to probe different indoor sources in a controlled and reproducible manner, leading to key insights on the contributions from sources/activities, the complex nature of the instrumentation deployed meant that measurements of occupied space were limited to those with scientists in them. Such large, multi-instrumented field studies are not suited for measuring indoor air quality while people undertake their normal activities and require unobtrusive instruments that can measure a suite of compounds. Many previous studies surveying occupied indoor spaces have relied on

passive samplers[75], as they are inexpensive, quantitative, unobtrusive, and safe to deploy in occupied spaces. The major disadvantage with passive samplers is their low time resolution, with sampling times of several days typically needed, which can make it difficult to fully capture the role and frequency of dynamic sources.

The tN_r instrument presented in this work strives to occupy a fruitful middle ground with its small footprint, safe (no dangerous chemicals required), insulated oven, quiet and automated operation making it suitable for measurements in both occupied and unoccupied indoor spaces. The tN_r instrument can be set up to measure without any operator input for several days and so can be used continuously in occupied indoor areas. Thus, it is ideal for surveying the indoor air quality contributions of a broad range N_r species across different environments, such as domestic residences, offices, and public buildings, without the need for multiple instruments targeting individual N_r species. The assembled inlet around a standard NO_x analyser also substantially reduces the cost to gain significant insight into the dynamics of many N_r species. Furthermore, the high time resolution of the tN_r instrument means that it can capture dynamic variability on the order of 20 minutes in N_r species levels and quantify the contributions from different sources, unlike passive samplers. Future work could focus on improving the tN_r instrument time resolution and could include the addition of a second chemiluminescence NO_x analyser, to enable simultaneous measurements of two pathways (Table 1). This could result in the instrument duty cycle being halved, and allow for differential measurements ($N_{r,acid}$ and $N_{r,base}$) during periods of dynamic variability. Improving the stability of the baseline through the tN_r oven could also be the focus of future work, which could be achieved by an automated cleaning with zero air when not in use (i.e. during NO_x pathway measurements) to minimize baseline contributions originating from the Pt catalyst.

Indoors, N_r species concentrations are high and a key driver of indoor air quality. This new tN_r instrument allows for a detailed survey of N_r species and can quickly visit several locations. Its mass-balance approach means that this instrument is also capable of identifying environments with unexpected distributions of N_r fractions that can stimulate more in-depth analysis in future fieldwork intensives like HOMChem. This is well illustrated in the proof-of-concept measurements in the kitchen, where NO_x, HONO and $N_{r,base}$ were unable to account for all the measured tN_r, pointing to a substantial missing fraction in the kitchen. Future work will identify the species contributing to this 'missing' tN_r fraction, using co-located measurements. Overall, the tN_r instrument can determine the emissions and sources of N_r species indoors and safely explore the unknown chemistry of indoor environments.

Author Contributions

Conceptualization and Funding: TV. Investigation: LRC, ML, LS. Methodology, software, data curation, formal analysis: LRC and ML. Writing – original draft: LRC and ML. Writing – editing: All authors.

Conflicts of Interest

There are no conflicts of interest to declare.

Acknowledgements

We thank CJ Young for the loan of the EC9841 during the kitchen observations. We thank the building operators, facilities managers, and kitchen staff for access to: the observation space, operations and sales logs, and ventilation data. ML acknowledges support through the Harold I. Schiff award in

atmospheric chemistry. LS acknowledges support through an Ontario Graduate Scholarship, the Charles Hantho award in atmospheric chemistry, and an Enbridge Graduate Award. This work was funded by the Alfred P. Sloan Foundation CIE Program (G-2018-11062, G-2018-11051), and NSERC Discovery Grants and Discovery Launch Supplement (RGPIN-2020-06166 and DGECR-2020-00186).

References

1 J. A. Logan, Nitrogen oxides in the troposphere: Global and regional budgets, *J. Geophys. Res. Ocean.*, 1983, **88**, 10785–10807.

2 N. Friedrich, I. Tadic, J. Schuladen, J. Brooks, E. Darbyshire, F. Drewnick, H. Fischer, J. Lelieveld and J. N. Crowley, Measurement of NOx and NOy with a thermal dissociation cavity ring-down spectrometer (TD-CRDS): instrument characterisation and first deployment, *Atmos. Meas. Tech.*, 2020, **13**, 5739–5761.

3 J. M. Roberts, C. E. Stockwell, R. J. Yokelson, J. de Gouw, Y. Liu, V. Selimovic, A. R. Koss, K. Sekimoto, M. M. Coggon, B. Yuan, K. J. Zarzana, S. S. Brown, C. Santin, S. H. Doerr and C. Warneke, The nitrogen budget of laboratory-simulated western US wildfires during the FIREX 2016 Fire Lab study, *Atmos. Chem. Phys.*, 2020, **20**, 8807–8826.

4 R. S. Park, S. Lee, S.-K. Shin and C. H. Song, Contribution of ammonium nitrate to aerosol optical depth and direct radiative forcing by aerosols over East Asia, *Atmos. Chem. Phys.*, 2014, **14**, 2185–2201.

5 J. C. Neff, E. A. Holland, F. J. Dentener, W. H. McDowell and K. M. Russell, The origin, composition and rates of organic nitrogen deposition: A missing piece of the nitrogen cycle?, *Biogeochemistry*, 2002, **57**, 99–136.

6 S. E. Cornell, Atmospheric nitrogen deposition: Revisiting the question of the importance of the organic component, *Environ. Pollut.*, 2011, **159**, 2214–2222.

7 A. Moravek, J. G. Murphy, A. Hrdina, J. C. Lin, C. Pennell, A. Franchin, A. M. Middlebrook, D. L. Fibiger, C. C. Womack, E. E. McDuffie, R. Martin, K. Moore, M. Baasandorj and S. S. Brown, Wintertime spatial distribution of ammonia and its emission sources in the Great Salt Lake region, *Atmos. Chem. Phys.*, 2019, **19**, 15691–15709.

8 S. Fuzzi, U. Baltensperger, K. Carslaw, S. Decesari, H. van der Gon, M. C. Facchini, D. Fowler, I. Koren, B. Langford, U. Lohmann, E. Nemitz, S. Pandis, I. Riipinen, Y. Rudich, M. Schaap, J. G. Slowik, D. V Spracklen, E. Vignati, M. Wild, M. Williams and S. Gilardoni, Particulate matter, air quality and climate: lessons learned and future needs, *Atmos. Chem. Phys.*, 2015, **15**, 8217–8299.

9 A. M. Avery, M. S. Waring and P. F. DeCarlo, Seasonal variation in aerosol composition and concentration upon transport from the outdoor to indoor environment, *Environ. Sci. Process. Impacts*, 2019, **21**, 528–547.

10 Y. Omelekhina, A. Eriksson, F. Canonaco, A. S. H. Prevot, P. Nilsson, C. Isaxon, J. Pagels and A. Wierzbicka, Cooking and electronic cigarettes leading to large differences between indoor and outdoor particle composition and concentration measured by aerosol mass spectrometry, *Environ. Sci. Process. Impacts*, 2020, **22**, 1382–1396.

11 I. Garbarienė, J. Pauraitė, D. Pashneva, A. Minderytė, K. Sarka, V. Dudoitis, L.

Davulienė, M. Gaspariūnas, V. Kovalevskij, D. Lingis, L. Bučinskas, J. Šapolaitė, Ž. Ežerinskis, G. Mainelis, J. Ovadnevaitė, S. Kecorius, K. Plauškaitė-Šukienė and S. Byčenkienė, Indoor-outdoor relationship of submicron particulate matter in mechanically ventilated building: Chemical composition, sources and infiltration factor, *Build. Environ.*, 2022, **222**, 109429.

12 J. Li, W. Xu, Z. Li, M. Duan, B. Ouyang, S. Zhou, L. Lei, Y. He, J. Sun, Z. Wang, L. Du and Y. Sun, Real-time characterization of aerosol particle composition, sources and influences of increased ventilation and humidity in an office, *Indoor Air*, 2021, **31**, 1364–1376.

13 N. Gysel, P. Dixit, D. A. Schmitz, G. Engling, A. K. Cho, D. R. Cocker and G. Karavalakis, Chemical speciation, including polycyclic aromatic hydrocarbons (PAHs), and toxicity of particles emitted from meat cooking operations, *Sci. Total Environ.*, 2018, **633**, 1429–1436.

14 J. C. Ditto, J. P. D. Abbatt and A. W. H. Chan, Gas- and Particle-Phase Amide Emissions from Cooking: Mechanisms and Air Quality Impacts, *Environ. Sci. Technol.*, 2022, **56**, 7741–7750.

15 B. C. Berman, B. E. Cummings, A. M. Avery, P. F. DeCarlo, S. L. Capps and M. S. Waring, Simulating indoor inorganic aerosols of outdoor origin with the inorganic aerosol thermodynamic equilibrium model ISORROPIA, *Indoor Air*, 2022, **32**, e13075.

16 J. P. D. Abbatt and C. Wang, *Environ. Sci. Process. Impacts*, 2020, 22, 25–48.

17 C. Wang, D. B. Collins, C. Arata, A. H. Goldstein, J. M. Mattila, D. K. Farmer, L. Ampollini, P. F. DeCarlo, A. Novoselac, M. E. Vance, W. W. Nazaroff and J. P. D. Abbatt, Surface reservoirs dominate dynamic gas-surface partitioning of many indoor air constituents, *Sci. Adv.*, 2020, **6**, eaay8973.

18 C. Wang, B. Bottorff, E. Reidy, C. M. F. Rosales, D. B. Collins, A. Novoselac, D. K. Farmer, M. E. Vance, P. S. Stevens and J. P. D. Abbatt, Cooking, Bleach Cleaning, and Air Conditioning Strongly Impact Levels of HONO in a House, *Environ. Sci. Technol.*, , DOI:10.1021/acs.est.0c05356.

19 L. Ampollini, E. F. Katz, S. Bourne, Y. Tian, A. Novoselac, A. H. Goldstein, G. Lucic, M. S. Waring and P. F. DeCarlo, Observations and Contributions of Real-Time Indoor Ammonia Concentrations during HOMEChem, *Environ. Sci. Technol.*, 2019, **53**, 8591–8598.

20 M. Li, C. J. Weschler, G. Bekö, P. Wargocki, G. Lucic and J. Williams, Human Ammonia Emission Rates under Various Indoor Environmental Conditions, *Environ. Sci. Technol.*, 2020, **54**, 5419–5428.

21 J. M. Mattila, P. S. J. Lakey, M. Shiraiwa, C. Wang, J. P. D. Abbatt, C. Arata, A. H. Goldstein, L. Ampollini, E. F. Katz, P. F. DeCarlo, S. Zhou, T. F. Kahan, F. J. Cardoso-Saldaña, L. H. Ruiz, A. Abeleira, E. K. Boedicker, M. E. Vance and D. K. Farmer,

Multiphase Chemistry Controls Inorganic Chlorinated and Nitrogenated Compounds in Indoor Air during Bleach Cleaning, *Environ. Sci. Technol.*, 2020, **54**, 1730–1739.

22 A. A. Angelucci, L. R. Crilley, R. Richardson, T. Valkenburg, P. S. Monks, J. M. Roberts, R. Sommariva and T. C. Vandenboer, Elevated levels of chloramines and chlorine detected near an indoor sports complex, *Environ. Sci. Process. Impacts*.

23 J. P. S. Wong, N. Carslaw, R. Zhao, S. Zhou and J. P. D. Abbatt, Observations and impacts of bleach washing on indoor chlorine chemistry, *Indoor Air*, 2017, **27**, 1082–1090.

24 E. C. Hall, S. R. Haines, K. Marciniak, A. H. Goldstein, R. I. Adams, K. C. Dannemiller and P. K. Misztal, Varying humidity increases emission of volatile nitrogen-containing compounds from building materials, *Build. Environ.*, 2021, **205**, 108290.

25 S. Robbana-Barnat, M. Rabache, E. Rialland and J. Fradin, Heterocyclic amines: occurrence and prevention in cooked food., *Environ. Health Perspect.*, 1996, **104**, 280–288.

26 K. Kikugawa, Formation of mutagens, 2-amino-3, 8-dimethylimidazo [4, 5-# f] quinoxaline (MeIQx) and 2-amino-3, 4, 8-trimethylimidazo [4, 5-# f] quinoxaline (4, 8-DiMeIQx), in heated fish meats, *Mutat. Res. Mol. Mech. Mutagen.*, 1987, **179**, 5–14.

27 D. K. Farmer, M. E. Vance, J. P. D. Abbatt, A. Abeleira, M. R. Alves, C. Arata, E. Boedicker, S. Bourne, F. Cardoso-Saldaña, R. Corsi, P. F. DeCarlo, A. H. Goldstein, V. H. Grassian, L. Hildebrandt Ruiz, J. L. Jimenez, T. F. Kahan, E. F. Katz, J. M. Mattila, W. W. Nazaroff, A. Novoselac, R. E. O'Brien, V. W. Or, S. Patel, S. Sankhyan, P. S. Stevens, Y. Tian, M. Wade, C. Wang, S. Zhou and Y. Zhou, Overview of HOMEChem: House Observations of Microbial and Environmental Chemistry, *Environ. Sci. Process. Impacts*, 2019, **21**, 1280–1300.

28 Moravek, A., Vandenboer, Trevor C., Z. A. Finewax, Pagonis, D, B. Nault, W. L. Brown, Day, D. A., A. V. Handshy, Stark, H., Ziemann, P., Jimenez, J. L., de Gouw, Joost. and C. J. Young, Reactive Chlorine Emissions from Cleaning and Reactive Nitrogen Chemistry in an Indoor Athletic Facility, *Environ. Sci. Technol.*

29 T. C. VandenBoer, M. Z. Markovic, A. Petroff, M. F. Czar, N. Borduas and J. G. Murphy, Ion chromatographic separation and quantitation of alkyl methylamines and ethylamines in atmospheric gas and particulate matter using preconcentration and suppressed conductivity detection, *J. Chromatogr. A*, 2012, **1252**, 74–83.

30 B. K. Place, A. T. Quilty, R. A. Di Lorenzo, S. E. Ziegler and T. C. VandenBoer, Quantitation of 11 alkylamines in atmospheric samples: separating structural isomers by ion chromatography, *Atmos. Meas. Tech.*, 2017, **10**, 1061–1078.

31 C. E. Stockwell, A. Kupc, B. Witkowski, R. K. Talukdar, Y. Liu, V. Selimovic, K. J. Zarzana, K. Sekimoto, C. Warneke, R. A. Washenfelder, R. J. Yokelson, A. M.

Middlebrook and J. M. Roberts, Characterization of a catalyst-based conversion technique to measure total particulate nitrogen and organic carbon and comparison to a particle mass measurement instrument, *Atmos. Meas. Tech.*, 2018, **11**, 2749–2768.

32 R. D. Saylor, E. S. Edgerton, B. E. Hartsell, K. Baumann and D. A. Hansen, Continuous gaseous and total ammonia measurements from the southeastern aerosol research and characterization (SEARCH) study, *Atmos. Environ.*, 2010, **44**, 4994–5004.

33 O. Marx, C. Brümmer, C. Ammann, V. Wolff and A. Freibauer, TRANC; a novel fast-response converter to measure total reactive atmospheric nitrogen, *Atmos. Meas. Tech.*, 2012, **5**, 1045–1057.

34 C. Ammann, V. Wolff, O. Marx, C. Brümmer and A. Neftel, Measuring the biosphere-atmosphere exchange of total reactive nitrogen by eddy covariance, *Biogeosciences*, 2012, **9**, 4247–4261.

35 A. J. Prenni, E. J. T. Levin, K. B. Benedict, A. P. Sullivan, M. I. Schurman, K. A. Gebhart, D. E. Day, C. M. Carrico, W. C. Malm, B. A. Schichtel, J. L. Collett and S. M. Kreidenweis, Gas-phase reactive nitrogen near Grand Teton National Park: Impacts of transport, anthropogenic emissions, and biomass burning, *Atmos. Environ.*, 2014, **89**, 749–756.

36 L. Thöni, E. Seitler, A. Blatter and A. Neftel, A passive sampling method to determine ammonia in ambient air, *J. Environ. Monit.*, 2003, **5**, 96–99.

37 M. J. Roadman, J. R. Scudlark, J. J. Meisinger and W. J. Ullman, Validation of Ogawa passive samplers for the determination of gaseous ammonia concentrations in agricultural settings, *Atmos. Environ.*, 2003, **37**, 2317–2325.

38 M. A. Puchalski, M. E. Sather, J. T. Walker, C. M. B. Lehmann, D. A. Gay, J. Mathew and W. P. Robarge, Passive ammonia monitoring in the United States: Comparing three different sampling devices, *J. Environ. Monit.*, 2011, **13**, 3156–3167.

39 D. Key, J. Stihle, J.-E. Petit, C. Bonnet, L. Depernon, O. Liu, S. Kennedy, R. Latimer, M. Burgoyne, D. Wanger, A. Webster, S. Casunuran, S. Hidalgo, M. Thomas, J. A. Moss and M. M. Baum, Integrated method for the measurement of trace nitrogenous atmospheric bases, *Atmos. Meas. Tech.*, 2011, **4**, 2795–2807.

40 P. S. J. Lakey, Y. Won, D. Shaw, F. F. Østerstrøm, J. Mattila, E. Reidy, B. Bottorff, C. Rosales, C. Wang, L. Ampollini, S. Zhou, A. Novoselac, T. F. Kahan, P. F. DeCarlo, J. P. D. Abbatt, P. S. Stevens, D. K. Farmer, N. Carslaw, D. Rim and M. Shiraiwa, Spatial and temporal scales of variability for indoor air constituents, *Commun. Chem.*, 2021, **4**, 110.

41 N. Zannoni, P. S. J. Lakey, Y. Won, M. Shiraiwa, D. Rim, C. J. Weschler, N. Wang, L. Ernle, M. Li, G. Bekö, P. Wargocki and J. Williams, The human oxidation field, *Science (80-.).*, 2022, **377**, 1071–1077.

42 Ecotech, *Serinus 40 user manual*, 2.2.

43 M. J. Navas, A. M. Jiménez and G. Galán, Air analysis: determination of nitrogen compounds by chemiluminescence, *Atmos. Environ.*, 1997, **31**, 3603–3608.

44 J. G. Murphy, D. A. Day, P. A. Cleary, P. J. Wooldridge, D. B. Millet, A. H. Goldstein and R. C. Cohen, The weekend effect within and downwind of Sacramento – Part 1: Observations of ozone, nitrogen oxides, and VOC reactivity, *Atmos. Chem. Phys.*, 2007, **7**, 5327–5339.

45 M. Lao, L. R. Crilley, L. Salehpoor, T. C. Furlani, I. Bourgeois, J. A. Neuman, A. W. Rollins, P. R. Veres, R. A. Washenfelder, C. C. Womack, C. J. Young and T. C. VandenBoer, A portable, robust, stable, and tunable calibration source for gas-phase nitrous acid (HONO), *Atmos. Meas. Tech.*, 2020, **13**, 5873–5890.

46 S. Zhou, C. J. Young, T. C. VandenBoer, S. F. Kowal and T. F. Kahan, Time-Resolved Measurements of Nitric Oxide, Nitrogen Dioxide, and Nitrous Acid in an Occupied New York Home, *Environ. Sci. Technol.*, 2018, **52**, 8355–8364.

47 W. Winberry Jr, T. Ellestad and R. Stevens, *Compendium method for the determination of inorganic compounds in ambient air: compendium method IO-4.2: determination of reactive acidic and basic gases and strong acidity of atmospheric fine particles (< 2.5 um)*, EPA/625/R-96/010a. US Environmental Protection Agency, Cincinnati, OH, 1999.

48 M. Brauer, P. B. Ryan, H. H. Suh, P. Koutrakis, J. D. Spengler, N. P. Leslie and I. H. Billick, Measurements of nitrous acid inside two research houses, *Environ. Sci. Technol.*, 1990, **24**, 1521–1527.

49 M. L. Fischer, D. Littlejohn, M. M. Lunden and N. J. Brown, Automated measurements of ammonia and nitric acid in indoor and outdoor air, *Environ. Sci. Technol.*, 2003, **37**, 2114–2119.

50 F. Vichi, L. Mašková, M. Frattoni, A. Imperiali and J. Smolík, Simultaneous measurement of nitrous acid, nitric acid, and nitrogen dioxide by means of a novel multipollutant diffusive sampler in libraries and archives, *Herit. Sci.*, 2016, **4**, 4.

51 N. Carslaw, A new detailed chemical model for indoor air pollution, *Atmos. Environ.*, 2007, **41**, 1164–1179.

52 S. R. Jackson, J. C. Harrison, J. E. Ham and J. R. Wells, A chamber study of alkyl nitrate production formed by terpene ozonolysis in the presence of NO and alkanes, *Atmos. Environ.*, 2017, **171**, 143–148.

53 W. W. Nazaroff and C. J. Weschler, Indoor acids and bases, *Indoor Air*, 2020, **30**, 559–644.

54 X. Ge, A. S. Wexler and S. L. Clegg, Atmospheric amines – Part I. A review, *Atmos. Environ.*, 2011, **45**, 524–546.

55 L. Salehpoor and T. C. Vandenboer, A highly selective, sensitive, and accurate ion chromatographic method with a conductivity detection for quantitative analysis of alkylamines in the aerosol and gas phases, *Anal. Methods*.

56 M. Lao and L. Crilley, tNr instrument software, https://github.com/data-lao/tNrInstrument.

57 S. Zhou, C. J. Young, T. C. VandenBoer and T. F. Kahan, Role of location, season, occupant activity, and chemistry in indoor ozone and nitrogen oxide mixing ratios, *Environ. Sci. Process. Impacts*, 2019, **21**, 1374–1383.

58 A. Moravek, S. Singh, E. Pattey, L. Pelletier and J. G. Murphy, Measurements and quality control of ammonia eddy covariance fluxes: a new strategy for high-frequency attenuation correction, *Atmos. Meas. Tech.*, 2019, **12**, 6059–6078.

59 R. A. Ellis, J. G. Murphy, E. Pattey, R. van Haarlem, J. M. O'Brien and S. C. Herndon, Characterizing a Quantum Cascade Tunable Infrared Laser Differential Absorption Spectrometer (QC-TILDAS) for measurements of atmospheric ammonia, *Atmos. Meas. Tech.*, 2010, **3**, 397–406.

60 T. C. VandenBoer, S. S. Brown, J. G. Murphy, W. C. Keene, C. J. Young, A. A. P. Pszenny, S. Kim, C. Warneke, J. A. de Gouw and J. R. Maben, Understanding the role of the ground surface in HONO vertical structure: High resolution vertical profiles during NACHTT-11, *J. Geophys. Res. Atmos.*, 2013, **118**, 10–155.

61 D. Pagonis, J. E. Krechmer, J. de Gouw, J. L. Jimenez and P. J. Ziemann, Effects of gas–wall partitioning in Teflon tubing and instrumentation on time-resolved measurements of gas-phase organic compounds, *Atmos. Meas. Tech.*, 2017, **10**, 4687–4696.

62 X. Liu, B. Deming, D. Pagonis, D. A. Day, B. B. Palm, R. Talukdar, J. M. Roberts, P. R. Veres, J. E. Krechmer, J. A. Thornton, J. A. de Gouw, P. J. Ziemann and J. L. Jimenez, Effects of gas--wall interactions on measurements of semivolatile compounds and small polar molecules, *Atmos. Meas. Tech.*, 2019, **12**, 3137–3149.

63 M. E. Monge, B. D'Anna and C. George, Nitrogen dioxide removal and nitrous acid formation on titanium oxide surfaces-an air quality remediation process?, *Phys. Chem. Chem. Phys.*, 2010, **12**, 8991–8998.

64 S. S. Park, J. H. Hong, J. H. Lee, Y. J. Kim, S. Y. Cho and S. J. Kim, Investigation of nitrous acid concentration in an indoor environment using an in-situ monitoring system, *Atmos. Environ.*, , DOI:10.1016/j.atmosenv.2008.05.023.

65 N. A. Mullen, J. Li, M. L. Russell, M. Spears, B. D. Less and B. C. Singer, Results of the California Healthy Homes Indoor Air Quality Study of 2011-2013: Impact of natural gas appliances on air pollutant concentrations, *Indoor Air*, 2016, **26**, 231–245.

66 B. C. Singer, R. Z. Pass, W. W. Delp, D. M. Lorenzetti and R. L. Maddalena, Pollutant concentrations and emission rates from natural gas cooking burners without and with range hood exhaust in nine California homes, *Build. Environ.*, 2017, **122**, 215–229.

67 X. Zhou, Y. He, G. Huang, T. D. Thornberry, M. A. Carroll and S. B. Bertman, Photochemical production of nitrous acid on glass sample manifold surface,

Geophys. Res. Lett., 2002, **29**, 5–8.

68 J. J. Schwab, Y. Li, M.-S. Bae, K. L. Demerjian, J. Hou, X. Zhou, B. Jensen and S. C. Pryor, A Laboratory Intercomparison of Real-Time Gaseous Ammonia Measurement Methods, *Environ. Sci. Technol.*, 2007, **41**, 8412–8419.

69 P. Gregoire, University of Toronto, 2013.

70 J. A. Neuman, T. B. Ryerson, L. G. Huey, R. Jakoubek, J. B. Nowak, C. Simons and F. C. Fehsenfeld, Calibration and Evaluation of Nitric Acid and Ammonia Permeation Tubes by UV Optical Absorption, *Environ. Sci. Technol.*, 2003, **37**, 2975–2981.

71 A. M. H. van der Veen, J. I. T. van Wijk, K. Harris, C. Goodman, J. Hodges, S. Uehara, J. H. Kang, Y. D. Kim, D. H. Kim, S. Lee, D. R. Worton, S. Bartlett, S. van Aswegen, P. J. Brewer, O. V Efremova, T. Zhang, D. Wang, Q. Han, Z. Zeyi, M. Iturrate-Garcia, C. Pascale and B. Niederhauser, International comparison CCQM-K117 ammonia, *Metrologia*, 2021, **58**, 8017.

72 T. Macé, M. Iturrate-Garcia, C. Pascale, B. Niederhauser, S. Vaslin-Reimann and C. Sutour, Air pollution monitoring: development of ammonia (NH$_{3}$) dynamic reference gas mixtures at nanomoles per mole levels to improve the lack of traceability of measurements, *Atmos. Meas. Tech.*, 2022, **15**, 2703–2718.

73 N. Wang, L. Ernle, G. Bekö, P. Wargocki and J. Williams, Emission Rates of Volatile Organic Compounds from Humans, *Environ. Sci. Technol.*, 2022, **56**, 4838–4848.

74 C. J. Weschler and N. Carslaw, Indoor Chemistry, *Environ. Sci. Technol.*, 2018, **52**, 2419–2428.

75 F. Villanueva, M. Ródenas, A. Ruus, J. Saffell and M. F. Gabriel, Sampling and analysis techniques for inorganic air pollutants in indoor air, *Appl. Spectrosc. Rev.*, 2022, **57**, 531–579.